Optimized Ionic Liquids for Toluene Absorption

Jorge Bedia, Elia Ruiz, Juan de Riva, Victor R. Ferro, Jose Palomar, and Juan Jose Rodriguez
Sección de Ingeniería Química (Dept. de Química Física Aplicada), Universidad Autónoma de Madrid, Cantoblanco, 28049 Madrid, Spain

DOI 10.1002/aic.13926
Published online October 18, 2012 in Wiley Online Library (wileyonlinelibrary.com).

Conductor-like-screening model for real solvents (COSMO-RS) method was used to analyze the solute-solvent interactions and to screen Henry's law constant of toluene over 272 ionic liquids (ILs), to select high-capacity absorbents. Thermogravimetric experiments were carried out to evaluate the toluene absorption by selected ILs at different temperatures and atmospheric pressure. Experimental equilibrium data were found in good agreement with COSMO-RS predictions. Complete desorption of toluene by N_2 stripping was achieved, indicating an easy regeneration. The kinetic curves were described by a phenomenological diffusion model, obtaining effective diffusivities in reasonable concordance with those calculated by Wilke–Chang correlation. The separation process with selected ILs was modeled by Aspen Plus and a comparison with organic absorbents was carried out. Equilibrium- and rate-based simulations were used to analyze the importance of thermodynamics and kinetics in toluene absorption by ILs. Current computational-experimental research allowed selecting a set of suitable ILs for toluene absorption. © 2012 American Institute of Chemical Engineers *AIChE J,* 59: 1648–1656, 2013

Keywords: ionic liquid, absorption, toluene, Henry constants, diffusivity, COSMO-RS, Aspen Plus, process simulation

Introduction

Volatile organic compounds (VOCs) are organic substances characterized by their high-vapor pressure at ambient temperature.[1] They are involved in atmospheric photochemical reactions and entail one of the most important groups of air pollutants emitted from chemical, petrochemical, and allied industries, leading to serious environmental problems (global warming, acid rain, and health hazard) and economical losses. Due to this, legislations such as Clean Air Act Amendments or European Economic Community (EEC) Directives limit the concentration levels for volatile organic compound emissions into atmosphere. The current methods used in VOC abatement (destructive- and recovery-based) include thermal or catalytic incineration, condensation, absorption, adsorption, membrane separation, and biological treatments, each with particular advantages and limitations.[2] Selection of an efficient VOC abatement technique depends on the concentration and the nature of the compound, the gas-stream flow rate, and other factors such as safety and economic considerations. Thermal oxidizers, commonly used for the destruction of VOCs, consume large amounts of natural gas to heat air and moisture, generating CO_2 and NO_X emissions, which have negative implications in global warming and air quality.[3] Catalytic oxidation processes[4,5] reduce the fuel consumption but have the problem of catalyst deactivation. Furthermore, the water vapor present in most of the gas streams and/or generated from VOCs oxidation frequently deactivates the inorganic catalytic systems. Biological treatments can represent a cost-effective solution for VOC removal, but they are not suitable when the microbial activity is limited by the slow VOC transfer from the gas phase to cell-containing aqueous phase.[6,7] It is also necessary to take into account that any destructive method eliminates the possibility of recovering the VOC. Adsorption of VOCs on different porous materials, such as, activated carbons or zeolites has been extensively studied in the literature[8,9] but its application may be limited because the moisture in the gas or the deposition of other compounds could block the adsorption sites making difficult the regeneration of the adsorbent.

Absorption can provide an effective solution for VOC removal from gas streams with further recovery. The key factor is the selection of an appropriate liquid absorbent.[10] For hydrophobic components, their low water solubility limits the absorption capacity in aqueous phase.[11] On the other hand, organic solvents [e.g., hexadecane and di-(2-ethyl) hexyladipate (DEHA) previously studied for toluene absorption[7]) present the disadvantage of their not negligible volatility. A strategy for improving the solute transfer to the aqueous phase is the addition of a nonaqueous solvent with high affinity for the solute, being silicone oils, n-alkanes, perfluorocarbons, and solid polymers widely used for this purpose.[12] Many of the requirements of VOC removal are fulfilled by an absorption system containing room-temperature ionic liquids (ILs).[3,7] ILs have received much attention in the last few years as potential candidates to substitute conventional flammable and volatile organic solvents in industrial processes.[13,14] Interest in ILs comes from their exceptional properties such as their extremely low-vapor pressure, nonflammability, and high thermostability.[13,15] Moreover, an important

Additional Supporting Information may be found in the online version of this article.

Correspondence concerning this article should be addressed to J. Palomar at pepe.palomar@uam.es.

feature of these solvents is the possibility of designing ILs with the required properties for a particular application by tuning the structure of the ions, hence the term "designer solvents."[16,17] Owing to these specific properties, ILs have generated significant interest across a wide variety of engineering applications, including their use as absorbents in gas separation processes,[18,19] such as CO_2 capture,[20,21] absorption of SO_2,[22,23] NH_3,[24–26] hydrofluorocarbons,[27,28] propylene,[29,30] or VOCs as dimethylsulfide, dimethyldisulfide, and toluene.[7] In this last reference, the high affinity of conventional imidazolium-based ILs for VOCs compounds was confirmed, being the partition coefficients in [bmim][PF_6] and [bmim][NTf_2] comparable or higher than those of typical organic solvents.[7] However, to the best of our knowledge, no systematic investigations on VOCs affinity toward a wide variety of ILs have been reported so far. For this purpose, computational methods to estimate thermodynamic properties are of great utility for selecting the best cation-anion combinations for a specific IL application.[25] The conductor-like-screening model for real solvents (COSMO-RS) model developed by Klamt et al.[31] is regarded as a valuable method for predicting the thermodynamic properties of ILs mixtures on the basis of quantum chemical calculations for the individual molecules,[32] providing an unique *a priori* computational tool for designing ILs with specific properties.[33–35] In fact, several publications have demonstrated the general suitability of COSMO-RS method to predict properties of IL systems, including the solubilities and Henry's law constants of several gases in ILs.[25,26,36,37] Moreover, an important feature is that the different intermolecular interactions between the mixture components can be quantified by COSMO-RS, contributing to the rational selection of ILs with improved characteristics for specific applications.[38,39] Indeed, in previous works released by our research group,[25,26,36,37] ILs with optimum characteristics for CO_2 and NH_3 absorption were selected, on the basis of a COSMO-RS analysis performed for the excess enthalpies of solute-IL mixtures and the COSMO-RS description of the intermolecular solute-IL interactions.

The aim of this work is to propose optimized ILs with high capacities and adequate properties for absorbing toluene. To accomplish that, a research strategy based on a three-step procedure was developed. First, a computational thermodynamic analysis using COSMO-RS molecular simulation method is performed among 272 ILs to select a set of solvents with convenient properties as toluene absorbents. Second, experiments are conducted to evaluate the thermodynamics and kinetics of toluene absorption. Thus, absorption-desorption rate curves over selected ILs are obtained by thermogravimetric experiments at different temperatures and atmospheric pressure. As a result, new thermodynamic and kinetic experimental data of interest for toluene absorption by ILs, such as gas-liquid equilibrium data and diffusivities, have been obtained and compared to the available data and calculated values. Third, toluene absorption was modeled in Aspen Plus v 7.3 at the operating conditions experimentally tested by using equilibrium- and rate-based columns (RADFRAC model).[40] Recently, our group showed[41,42] that IL compounds can be successfully created as new (pseudo)components in Aspen Plus by transferring COSMO-RS results to process simulator. In addition, it was demonstrated that COSMOSAC property model[43,44] can support the property prediction of the pure ILs and their mixtures with organic compounds in process simulations. This procedure allows the simulation of separation processes based on new components initially not available in the simulator database (as it is the case of ILs). In this work, the simulation of toluene absorption in selected ILs and in other conventional toluene absorbents (as hexadecane and DEHA) using Aspen Plus is first validated by comparison to our own experimental gas-liquid equilibrium and kinetic data. Then, rate-based calculations are performed to estimate the absorption of toluene in tray and packed columns at fixed gas/liquid mass ratio and operational conditions. The recovery of toluene achieved using rate-based approach is compared to the separation obtained using an ideal single equilibrium stage, which allows analyzing the importance of kinetics and thermodynamics in toluene absorption. In this way, a set of optimized ILs are confidently evaluated as potential candidates in absorption processes for the removal and recovery of toluene (a representative aromatic VOC) from gaseous streams.

Procedure

Molecular simulation: Computational details of COSMO-RS calculations

The molecular geometry of toluene, hexadecane, and cations and anions of ILs (see IL names and abbreviations in Supporting Information, Table S1) was optimized at B3LYP/6-31++G** computational level in the ideal gas phase using the quantum chemical Gaussian03 package.[45] A molecular model of independent counterions was applied in COSMO-RS calculations, where the IL is treated as equimolar mixture of cation and anion. Vibrational frequency calculations were performed in each case to confirm the presence of an electronic energy minimum. After that, the standard procedure was applied for COSMO-RS calculations, which consists of two steps: first, Gaussian03 was used to compute the COSMO files. The ideal screening charges on the molecular surface for each species were calculated by the continuum solvation COSMO model using BVP86/TZVP/DGA1 level of theory. Subsequently, COSMO files were used as input in COSMOtherm statistical thermodynamic calculations. The version C21_0111 of the COSMOthermX program package[46] and its implicit (BP_TZVP_ C21_0111) parameterization were used to accomplish the calculations of the σ-profiles of pure compounds as well as thermodynamic properties such as Henry's law constants for toluene in ILs and detailed contributions to excess enthalpies in equimolar toluene-IL mixtures.

Materials

Toluene (purity >99.8%) was purchased from Sigma-Aldrich and used without further purification. The ILs tested as absorbents were the following [dcmim][NTf_2], [omim][NTf_2], [hxmim][NTf_2], [bmim][NTf_2], [emim][NTf_2], [dcmim][Cl], [dcmim][BF_4], [emim][$C_2H_5SO_4$], and [bmim][BF_4] supplied by Ionic Liquid Technologies, in the highest purity available (purity >97–98%). All the ILs were used also without further purification. Before each experiment, the ILs was dried under vacuum (10^{-3} Torr) at 298 K over at least 24 h. This procedure ensures working with ILs with very low water content (<250 ppm).[25,26] Therefore, the water should not significantly affect the absorption capacity, as in fact we have found.[25,26] Table 1 collects the density and viscosity values reported in the literature[47–49] for the different ILs used in this work. As can be seen, the properties measured by us for the IL used as reference [bmim][BF_4][25] are fairly close to the reported by other authors.[50]

Table 1. Density and Viscosity of the ILs Reported in Literature

IL	Temperature (K)	Density (kg/m^3)	Viscosity (mPa s)	References
[dcmim][NTf_2]	293	1282	141	47
	303	1278	84	
	313	1274	54	
[omim][NTf_2]	293	1327	115	48
	303	1320	71	
	313	1307	46	
[hxmim][NTf_2]	293	1376	91	47
	303	1367	56	
	313	1358	36	
[bmim][NTf_2]	293	1441	63	49
	303	1432	40	
	313	1424	27	
[emim][NTf_2]	293	1524	41	47
	303	1514	28	
	313	1506	20	
[dcmim][BF_4]	293	1072	928	48
	303	1067	456	
	313	1060	248	
[emim][$C_2H_5SO_4$]	293	1241	111	49
	303	1234	75	
	313	122	53	
[bmim][BF_4]	293	1203/1208	123/107	25/50
	303	−/1201	−/72	
	313	1189/1195	48/50	

Absorption/desorption experiments

Figure 1 shows a scheme of the setup used for toluene equilibrium and kinetic absorption experiments. They were carried out in a thermogravimetric analyzer (TGA/SDTA851^e Mettler Toledo International Inc.) at atmospheric pressure and temperatures of 293, 303, and 313 K using around 20 mg of IL previously dried as described before. The balance has a weight range of 0–1000 mg with a resolution of 0.1 μg. The temperature of the sample was maintained constant with an external thermostatized bath (Huber minisat 125). Toluene inlet concentration was set by saturation of a nitrogen flow through a saturator at a controlled temperature. Gas-liquid equilibrium data of toluene in ILs were obtained by setting the partial pressure of toluene in the toluene/N_2 gas flow (100 Ncm^3/min) and monitoring the increment on weight of the sample. Blank experiments were carried out with neat N_2 gas and no weight increase of the IL samples was detected, consistently with the reported negligible solubility of N_2 in imidazolium-based IL ($<10^{-3}$ molar fraction at 1 atm and 40°C).[51] It was considered that the IL and the gas have reached equilibrium when at constant pressure no further weight change was observed on time (weight change rate <0.001 mg h^{-1}).

The absorption–desorption rate curves were also obtained in the aforementioned thermogravimetric system. Toluene absorption was performed at an inlet toluene partial pressure of 2.0 kPa under continuous gas flow (100 Ncm^3/min) at 0.1 MPa. The increment of weight was monitored, and once the IL and the gas seem to have reached equilibrium (weight change rate <0.001 mg h^{-1}), desorption was carried out at the absorption temperature with continuous dry nitrogen flow (100 Ncm^3/min).

Process simulation details

In process simulations, IL new components were created as pseudocomponents through Aspen Plus (v 7.3) specifying their molecular weights, normal boiling temperatures, and densities. Additionally, the coefficients of the Andrade's equation for the viscosity-to-temperature dependency were specified. These coefficients were regressed from experimental data.[25,47,48,50] The remainder unknown properties of the IL pseudocomponents were estimated by the methods and models implicitly used in Aspen Plus. Toluene and nitrogen were selected as conventional components from the Aspen Plus ASPV73 PURE25 database. The COSMOSAC property model[44,52] as implemented by default in Aspen Plus was selected to estimate the activity coefficients of the components in the mixtures.[44] The molecular volumes and σ-profiles of the ILs, needed for specifying the COSMOSAC model, were set by the user, whereas those corresponding to the organic solvents were directly taken from the Aspen Plus' database. The information used for both creating IL pseudocomponents (normal boiling temperature and densities) and specifying the corresponding COSMOSAC property models were obtained from the previous COSMO-RS calculations by the COSMO-*therm*X (v C21_0111) program package assuming ion-paired structures (molecular CA model) for the ILs.

Toluene absorption was simulated with the RADFRAC model of Aspen Plus.[40] In rate-based absorption simulations: (i) toluene + IL mixtures were considered as nonreacting systems, (ii) diffusivities of the toluene in the IL phase were calculated by the Wilke–Chang equation as implemented in Aspen Plus (v 7.3), (iii) both trayed and packed columns were evaluated, (iv) dimensions of the tray and pack section were previously estimated by the tray- and pack-sizing utilities available in Aspen Plus, and (v) correlations used by default in Aspen Plus (v 7.3) to calculate the mass- and heat-transfer coefficients and interfacial areas in rate-based absorption simulations were employed here. Two rate-based absorption models have been used in this work:

One-Stage Contactor Column. It was considered for evaluating the absorptive capacity of different ILs using a gas feed with inlet toluene partial pressure of 2.0 kPa. In addition, it allows comparing the separation achieved using rate- and equilibrium-based approaches, to evaluate how the kinetics affect to the absorption process. In addition, Murphree tray efficiencies were also evaluated. The feed flows of the IL and gas were fixed at $L = 0.01$ and $G = 0.35$ kmol/h, respectively. A G/L of 35 value was selected because it allows observing significant deviations of toluene recovery from ideal equilibrium. The inlet streams were fed "on stage" according to Aspen Plus convention. Sieve tray dimensions were fixed at 0.3 m diameter and 0.15 m height.

Packed Bed Column. A more realistic absorption model of packed bed column was also considered in this study for the selected IL dcmimNTf_2 and commonly used conventional absorbents (DEHA and n-hexadecane). For the sake, comparison in an industrial-like approach, a column size

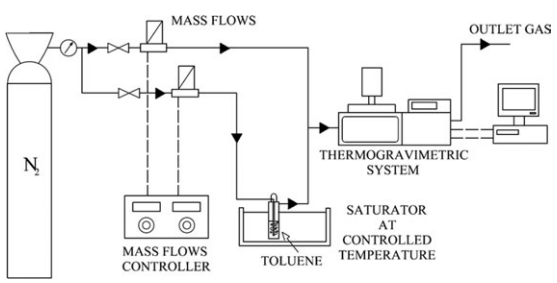

Figure 1. Schematic diagram of the atmospheric pressure system for toluene absorption.

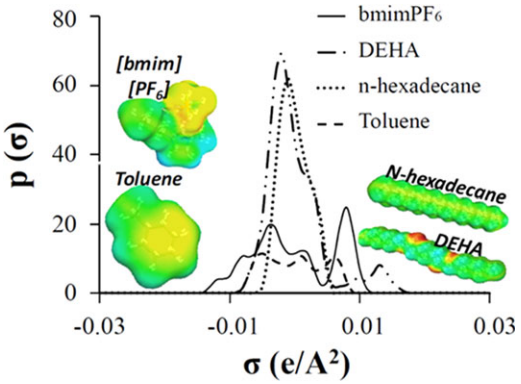

Figure 2. σ-Profiles and polarized charge surfaces of toluene and different solvents obtained by COSMO-RS.

[Color figure can be viewed in the online issue, which is available at wileyonlinelibrary.com.]

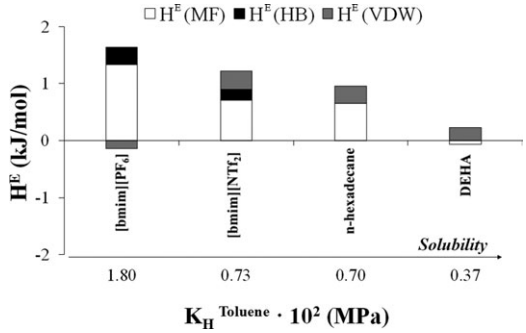

Figure 3. Description of the solvent effect on Henry's law constants of toluene at T = 298 K by using the interaction energies contributions [electrostatic, H(MF); Van der Waals, H(VDW), and hydrogen-bonding, H(HB)] to excess molar enthalpies of solute-solvent mixtures computed by COSMO-RS.

representative of a pilot plant unit (2 m height, 0.25 m diameter, and 15 mm ceramic Raschig rings) was selected. The G/L molar ratio was chosen taking DEHA as reference solvent for 90% recovery. The obtained G/L molar ratio (17) is in the range of values value commonly used in aromatics absorption with conventional organic solvents[53] and was maintained for the other two IL-based systems. The height equivalent to a theoretical plate (HETP) was calculated at those different conditions to characterize the packing efficiency, determined by the rate of the absorption process.

Results

COSMO-RS selection of ILs for toluene absorption

COSMO-RS method calculates the thermodynamic properties of fluid mixtures using the molecular surface polarity distributions of their individual compounds from quantum chemical calculations, data easily visualized in the histogram function σ-profile.[31] Figure 2 shows the σ-profile of toluene, which is dominated by a series of peaks located at the nonpolar region ($-0.0082 < \sigma < +0.0082$ e/Å^2). This neutral character of toluene anticipates predominant misfit (electrostatic) intermolecular interactions. Conversely, the σ-profile of conventional toluene absorbents, as DEHA or hexadecane[7], is also dominated by peaks located at the nonpolar region (Figure 2), which confirms the well-known solute-solvent affinity. In contrast, the ionic liquid previously used as toluene absorbent,[7] [bmim][PF_6], although it yields a significant peak at the nonpolar region, not only shows polarized charge corresponding to hydrogen groups of cation located at the hydrogen bond donor region $\sigma < -0.0082$ e/Å^2 but also shows the anion negative charge density located in the hydrogen-bond acceptor region $\sigma > 0.0082$ e/Å^2, which indicates the higher polar character of IL relative to solvents like DEHA or hexadecane and is consistent with the experimentally measured higher solubility of toluene in those solvents compared to [bmim][PF_6].[7]

In previous studies, COSMO-RS estimations for excess enthalpy, H^E, of solute-IL mixtures was successfully applied to analyze the gas-liquid equilibrium data in terms of the misfit, hydrogen bonding, and van der Waals intermolecular interactions

$$H^E = H^E(H\text{-}Bond) + H^E(Misfit) + H^E(VdW) \qquad (1)$$

Figure 3 shows the values of Henry's law constants for toluene in DEHA, n-hexadecane, and [bmim][PF_6] at T = 298 K together with interaction energy contributions to excess molar enthalpies of toluene-solvent system, both computed by COSMO-RS. It is observed that a decrease of repulsive interactions (positive H^E values) accompanies an increasing gas solubility of toluene (decreasing K_H values). As can be seen in that figure, organic solvents present less repulsive interactions than the ionic liquid [bmim][PF_6].

To design optimized ILs for toluene absorption, COSMO-RS method was here applied for predicting Henry's law constants (K_H) for toluene in 272 ILs at 298 K (collected in Supporting Information, Table S2). Thus, a computational screening was performed over ILs based on different cations (imidazolium, pyridinium, pyrrolidinium, phosphonium, and ammonium) and anions ([$C_6F_{18}P^-$], [$FeCl_4^-$], [$C_8H_{17}SO_4^-$], [NTF_2^-], [$BC_4N_4^-$], [Formate], [$CH_3CO_2^-$], [$CH_3SO_3^-$], [$CF_3CO_2^-$], [$C_2H_5SO_4^-$], [$C_4N_3^-$], [PF_6^-], [$CF_3SO_3^-$], [$CH_3SO_4^-$], [DCN^-], [NO_3^-], [BF_4^-]), being the K_H values mapped in Figure 4. It is observed that the toluene absorption capacity of ILs is determined by the selection of both cationic and anionic structures. Regarding the cation family effect, and focusing specially on the white region of the map

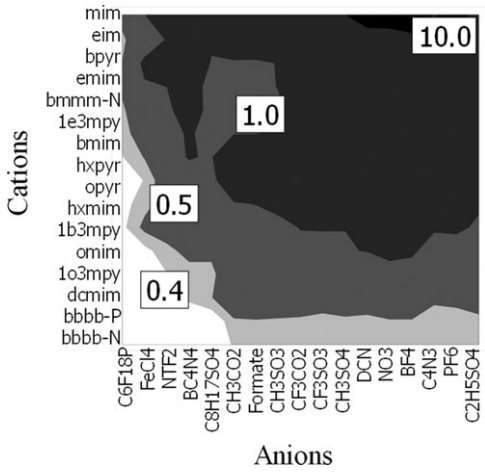

Figure 4. Screening of predicted Henry's law constants (10^2 MPa) for toluene in 272 ILs at T = 298 K calculated by COSMO-RS.

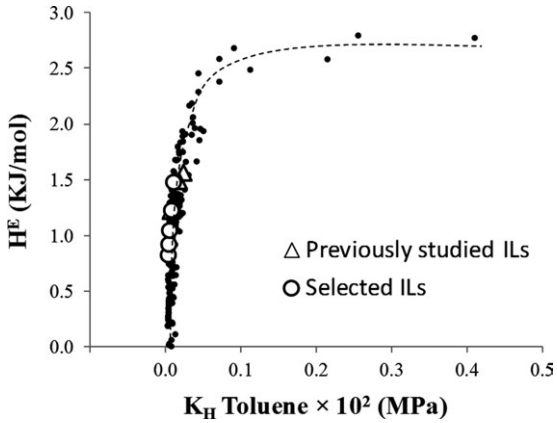

Figure 5. Excess molar enthalpies (H^E) of equimolar toluene-IL mixtures versus Henry's law constants (K_H) for toluene in >200 different ILs, both computed by COSMO-RS at 298 K.

(which corresponds to ILs whose toluene K_H values fall in the order of the benchmark absorbent DEHA), long chain imidazolium cations and tetra-substituted long chain phosphonium or ammonium cations seem to improve the capacity for absorbing toluene. However, taking into account the higher viscosity of ILs based on tetra-substituted long chain ammonium or phosphonium cations,[54–56] we decided to select ILs based on imidazolium cations for this study. On the other hand, Figure 4 indicates that highly halogenated hydrophobic anions—such as $[C_6F_{18}P^-]$, $[NTF_2^-]$, and $[FeCl_4^-]$—also improve the absorption of toluene.

In the following, computational analysis is focused on a set of commercially available imidazolium-based ILs with favorable thermodynamics for toluene absorption. Figure 5 compares excess enthalpy, H^E, for equimolar toluene-IL mixtures with Henry's law constant values for more than 200 different ILs (those with K_H vs. $<5{\cdot}10^{-3}$ MPa), both estimated by COSMO-RS. As a general trend, higher solubilities (decreasing K_H values) of toluene in ILs are associated to lower endothermicity (decreasing H^E values) of the mixtures. Analyzing the computational results of Figures 4 and 5, it was able to choose six selected ILs where the predicted values of toluene Henry's constant are lower than those for previously studied ILs in bibliography as toluene absorbents.[7] In addition, we decided to evaluate the suitability as toluene absorbent of an IL with relative low cost, based on ethylsulfate anion [emim][$C_2H_5SO_4$]. Figure 6 allows analyzing the absorption of toluene in these set of selected ILs in terms of the contributions of different intermolecular interactions to the H^E values of toluene-IL mixtures. It illustrates that electrostatic (Misfit) forces represent the main solute-solvent interactions, which enhance the solubility of toluene in IL when increases the length of alkyl chain, that is, the nonpolar character of the solvent.

Toluene absorption experiments

From COSMO-RS computational analysis, we selected the commercially available ILs [dcmim][NTf_2], [omim][NTf_2], [hxmim][NTf_2], [emim][NTf_2], [dcmim][BF_4], and [emim][$C_2H_5SO_4$] as promising potential solvents to be experimentally tested for toluene absorption. The results will be compared with those reported with [bmim][NTf_2][7] and the obtained with [bmim][BF_4] as reference conventional IL. Figure 7 shows the results of absorption equilibrium experiments performed using toluene/N_2 gas mixtures and [dcmim][NTf_2] (the IL with higher toluene solubility predicted by COSMO-RS) at atmospheric pressure and temperatures of 293, 303, and 313 K. For a initial toluene concentration of 20000 ppmv, [dcmim][NTf_2] absorbs at equilibrium a significant amount of 0.34 g of toluene per gram of IL at 293 K and 1 atm. Figure 7 confirms that, as expected, toluene solubilities increase with decreasing temperature and increasing toluene partial pressure. The Henry's law constant, K_H, could be calculated using the mole fraction of toluene in the IL and the equilibrium pressure, P, by

$$K_H = \lim_{x_{Tol}\to 0}\left(\frac{p}{x_{Tol}}\right) \tag{2}$$

This expression is rigorously applied to a pure toluene gas phase in contact with the IL. In our experimental conditions, we use a binary gas phase mixture of nitrogen and toluene. However, taking into account the low solubility of N_2 in imidazolium-based IL ($<10^{-3}$ molar fraction at 1 atm and 313 K)[51] and assuming a very low interaction between nitrogen and toluene molecules, the effect of nitrogen in the toluene absorption process can be neglected. Furthermore, the relation between the equilibrium pressure and the mole fraction of toluene is linear in the entire toluene mole fraction (Figure 7) at all the temperatures tested, despite the high values of toluene mole fraction reached in the IL. Considering these assumptions,[57,58] the slopes of linear fits of Figure 7 provide representative values of Henry's law constant (K_H) for toluene absorption in the selected IL [dcmim][NTf_2]. The resulting K_H values from

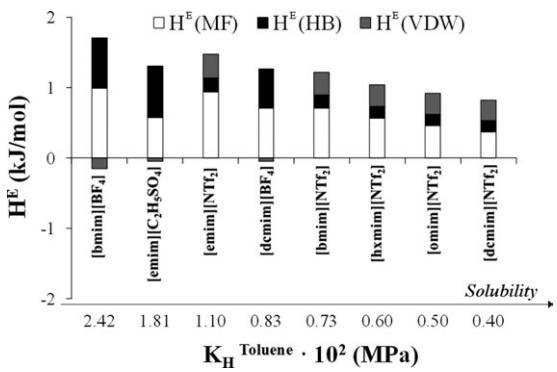

Figure 6. Henry's law constants for toluene in ILs vs. the excess molar enthalpies of toluene-IL mixtures at T = 298 K obtained by COSMO-RS.

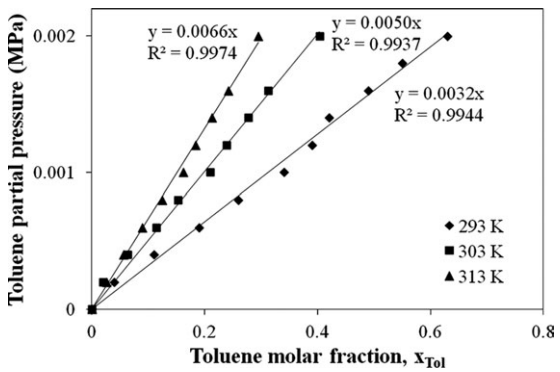

Figure 7. Equilibrium curves of toluene absorption on [dcmim][NTf_2] ILs measured at 293, 303, and 313 K and total 0.1 MPa.

Table 2. Henry's Law Constant (K_H) for Toluene Absorption in [dcmim][NTf_2] Estimated from Equilibrium Experiments and Predicted by COSMO-RS

Temperature	Experimental K_H (MPa)	COSMO-RS K_H (MPa)
293	0.0032	0.0031
303	0.0050	0.0049
313	0.0066	0.0078

experiments at different temperatures are in very good agreement with the predicted by COSMO-RS (see Table 2).

Figure 8 shows the absorption-desorption curves of toluene in (a) ILs with [NTf_2] anion and (b) other ILs, obtained by thermogravimetric measurements at 293 K and atmospheric pressure and a toluene partial pressure of 2.0 kPa. Similar curves were obtained at 303 and 313 K (Supporting Information, Figures S1 and S2), decreasing the absorption toluene with increasing temperatures for all the ILs analyzed, as expected. Figure 8a clearly shows a decrease in the amount of toluene absorbed at saturation as the length of the alkyl chain length of the imidazolium cation decreases. The lowest toluene absorption capacities correspond to ILs with less hydrophobic anions and shorter alkyl chains, [emim][$C_2H_5SO_4$] and [bmim][BF_4] ILs (Figure 8b), which show also the highest values of the predicted Henry's constant (Figure 6). As can be seen, the good correlation between the COSMO-RS predictions and the experimental toluene absorption capacities as can be seen in Figure 9, indicating the validity of K_H as thermodynamic parameter of reference to select ILs for toluene absorption processes.

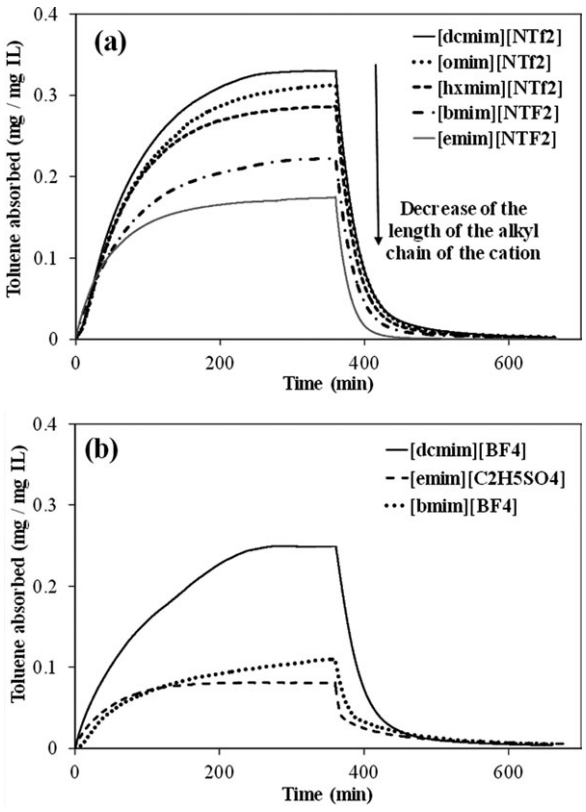

Figure 8. Toluene absorption-desorption curves at 293 K and atmospheric pressure in (a) ILs with [NTf_2] anion and (b) other ILs (toluene partial pressure of 2.0 kPa for absorption).

Desorption of toluene from the saturated IL is a key issue regarding potential applications. The desorption curves under continuous bare N_2 flow are included in Figure 8. Desorption of toluene was complete in all the cases, that is, all the toluene absorbed was desorbed at the absorption temperature, without the need of heating or vacuum which has been reported with other ILs.[59] Thus, complete regeneration would be possible by simple stripping at the same ambient-like absorption temperature.

To quantify the kinetics of toluene absorption in the different ILs, diffusion coefficients were estimated by applying a simplified mass diffusion model previously used for CO_2 absorption in ILs.[60–62] The process may be described by one-dimensional mass diffusion due to the local concentration difference. The toluene mass balance can be written as

$$\frac{\partial C}{\partial t} = D \cdot \frac{\partial^2 C}{\partial z^2} \tag{3}$$

with an initial condition $C = 0$ when $t = 0$ and $0 < z < L$ and boundary conditions (i) $C = C_s$ when $t > 0$ and $z = 0$ and (ii) $\partial C/\partial z = 0$ at $z = L$. C is the concentration of toluene dissolving in the IL as a function of time, t, and vertical location, z, L is the depth of IL in the container (estimated for each case using the weight of IL in the sample pot and the corresponding density value of IL reported in Table 1). D is the diffusion coefficient that is assumed constant and in this case must be taken as an "effective diffusion coefficient" because the toluene-IL liquid mixtures cannot be considered diluted solutions. The simplification of assuming diluted solutions has been previously used by other authors working with CO_2-ILs systems reaching even higher solute concentration than ours.[60] The experimentally measured toluene concentration (mass per unit volume) in IL at a given time corresponds to the space-averaged concentration, $\overline{C}$, at that time, which can be calculated from the equation

$$\overline{C} = \frac{1}{L}\int_0^L C dz \tag{4}$$

$$\overline{C} = C_s\left[1 - 2\sum_{n=0}^{\infty}\frac{\exp(-\lambda_n^2 Dt)}{L^2\lambda_n^2}\right] \tag{5}$$

Although this equation contains an infinite summation, only the first four terms are sufficient in practical applications. Fitting the experimental data to this equation, we obtained the

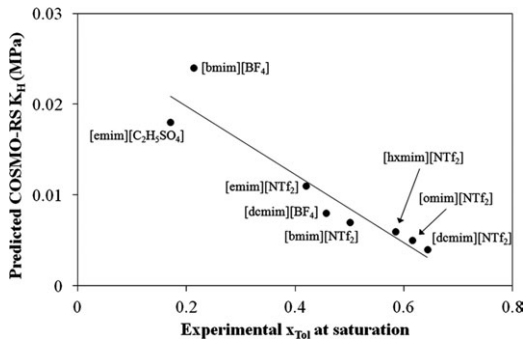

Figure 9. COSMO-RS predicted K_H values at 298 K vs. experimental toluene absorption capacities (molar fraction) obtained at 293 K, atmospheric pressure and 2 kPa toluene partial pressure.

Table 3. Effective Diffusion Coefficients of Toluene in ILs at Different Temperatures Obtained from Absorption Measurements and Estimated by Wilke–Chang Correlation

IL	Temperature (K)	$D \times 10^{11}$ (m^2/s)	R^2	$D \times 10^{11}$ (m^2/s) (Wilke–Chang)
[dcmim][NTf_2]	293	3.9	0.994	2.2
	303	7.5	0.996	3.8
	313	8.9	0.998	6.1
[omim][NTf_2]	293	3.8	0.994	2.6
	303	7.2	0.998	4.3
	313	9.0	0.992	6.8
[hxmim][NTf_2]	293	3.9	0.992	3.1
	303	7.1	0.995	5.2
	313	10.1	0.998	8.1
[bmim][NTf_2]	293	4.6	0.998	4.3
	303	7.8	0.995	7.0
	313	10.6	0.993	10.5
[emim][NTf_2]	293	5.5	0.996	6.3
	303	8.1	0.996	9.5
	313	10.7	0.992	13.6
[dcmim][BF_4]	293	3.76	0.999	2.5
	303	6.13	0.998	5.3
	313	9.86	1.000	10.0
[emim][$C_2H_5SO_4$]	293	6.50	0.998	1.8
	303	10.2	0.999	2.8
	313	11.0	0.995	4.1
[bmim][BF_4]	293	7.10	0.992	1.6
	303	8.97	0.998	2.9
	313	10.8	0.998	4.4

saturation concentration (C_s) and the diffusion coefficient (D) at given T and P. The fitting was performed by nonlinear regression. Table 3 summarizes the values of the effective diffusion coefficient of toluene in different ILs at the three absorption temperatures tested. The correlation coefficients (R^2) show fairly good values in all the cases ($R^2 > 0.99$). For comparison purposes, the values of D were tentatively estimated by the Wilke–Chang correlation, widely applied in bibliography to predict diffusion coefficients[63]

$$D = 7.4 \cdot 10^{-8} \frac{(\phi \cdot M_{IL})^{0.5} \cdot T}{\mu_{IL} \cdot V_{Toluene}{}^{0.6}} \quad (6)$$

where T is temperature (K), μ_{IL} and $V_{Toluene}$ are, respectively, the viscosity of IL (Table 1) and the molar volume of toluene at the corresponding temperature, M_{IL} is the molar mass of IL and ϕ is the association parameter (with value of 1, considering in this case IL as unassociated solvent). As can be seen in Table 3, there is a good agreement between the D values obtained from the absorption experiments and those estimated by Wilke–Chang correlation. The diffusion coefficients increase with the absorption temperature consistently with the decrease of the ILs viscosities (Table 1). It is also worth mentioning that, as a general trend, the effective diffusion coefficients increase when decreasing the length of the imidazolium cation alkyl chain of ILs containing the common anion [NTf_2], again, in agreement with the lower viscosity of the IL with shorter alkyl chain (Table 1). It should be indicated that the D values obtained in this work for the absorption of toluene in [bmim][BF_4] are in the order of magnitude of those previously reported for CO_2 with this IL.[60]

Process simulation results

In this section, the process simulator Aspen Plus v 7.3 was used for modeling and evaluating the absorption of toluene by ILs (favorable series with common anion NTf_2^-) in separation columns of different types. First, the eventual inclusion of ILs as new components in Aspen Plus was checked by comparing the experimental values of density, viscosity, toluene diffusivity, and toluene absorption equilibrium data for the IL tested to those predicted by Aspen Plus software using COSMOSAC property model. Supporting Information, Table S3 shows the good agreement between experimental and simulated property values for the five IL-toluene systems evaluated, demonstrating both the confidence of ILs implementation as pseudocomponents in Aspen Plus and the capacity of the COSMOSAC property model for estimating thermophysical and equilibrium properties of the mixtures (ILs + toluene).

The recovery of toluene at given operating conditions ($C_{Toluene}$ in gas: 2000 ppmv; $G/L = 35$ in mol, 298 K and 1 atm) was simulated in a single-stage contactor using both equilibrium- and rate-based approaches by RADFRAC in Aspen Plus. The results for rate-based one-stage absorption (Table 4) show that toluene recovery follows the general trend of gas-liquid equilibrium data reported before: DEHA > [dcmim][NTf_2] > [omim][NTf_2] > n-hexadecane > [hxmim][NTf_2] > [bmim][NTf_2] > [emim][NTf_2]. In addition, toluene separation in rate-based simulation is significantly enhanced at lower-temperatures for all the solvents considered, in spite of the lower diffusion coefficients (see Table 3). These results suggest that thermodynamics prevails over kinetics, thus being the determining factor in toluene absorption by the ILs tested under experimental conditions of this work.

Nevertheless, Figure 10a, which compares the percentage of recovered toluene by using rate- and equilibrium-based models for the IL series, suggests that the kinetics also influences toluene absorption by ILs. Remarkably, the more effective IL absorbents present the less favorable mass transfer properties and, as consequence, lower Murphree tray efficiencies (Figure 10b). This clearly points to the convenience of taking into account kinetic considerations in the selection

Table 4. Toluene Recoveries (%) and Murphree Tray Efficiencies for the Separation of Toluene by Absorption With ILs and Organic Solvents in a One-stage Contactor, Using Equilibrium and Rate-Based Models for Separation Column

	% Toluene Recovery								
	Rate-Based Model			Equilibrium Model			Murphree Tray Efficiency		
IL	293 K	303 K	313 K	293 K	303 K	313 K	293 K	303 K	313 K
[dcmim][NTf_2]	52.3	40.0	29.6	67.0	50.1	35.4	0.78	0.80	0.84
[omim][NTf_2]	48.3	36.3	26.5	61.9	45.0	31.2	0.78	0.81	0.85
[hxmim][NTf_2]	44.7	33.0	23.7	57.0	40.4	27.5	0.78	0.82	0.86
[bmim][NTf_2]	40.7	29.5	20.9	51.5	35.6	23.8	0.79	0.83	0.87
[emim][NTf_2]	35.4	25.1	17.5	44.1	29.5	19.5	0.80	0.85	0.90
n-Hexadecane	45.8	34.4	25.1	56.8	40.8	28.2	0.80	0.84	0.89
DEHA	64.7	52.6	41.0	81.0	66.3	50.2	0.78	0.80	0.82

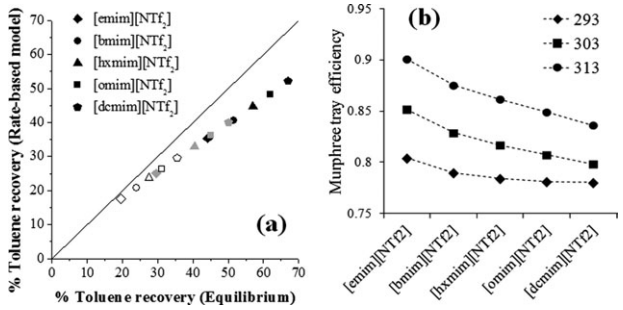

Figure 10. (a) Equilibrium- vs. rate-based toluene recovery values and (b) Murphree tray efficiencies using different ILs at 293, 303, and 313 K.

of both the IL solvent and the operating conditions. On the other hand, the one-stage absorption results (Table 4 and Figure 10) indicate that the selected IL [dcmim][NTf_2] could be a promising alternative to conventional organic absorbents, as n-hexadecane or DEHA.[7]

To evaluate this point, the absorption of toluene gas has been simulated in a packed column using [dcmim][NTf_2], n-heaxadecane and DEHA as absorbents, operating at 293 K and 1 atm with a molar *G*/*L* ratio of 17 and with the column dimensions described in the section Process simulation details. The main results are summarized in Table 5. As can be seen, toluene recovery and concentration in the exit gas stream when using [dcmim][NTf_2] as solvent present intermediate values to the conventional organic solvents, DEHA and n-hexadecane. It should be pointed out that the mass transfer efficiency of the packed column simultaneously depends on gas and liquid flow rate, density, viscosity, and diffusivity (see Supporting Information, Scheme 1S and Table 4S). Aspen Plus simulations provide lower HETP values, that is, higher mass transfer efficiency in this packed column, for the selected IL [dcmim][NTf_2] than for the organic solvents DEHA and n-hexadecane.

Conclusions

A computational-experimental strategy research was developed to select ILs with favorable properties for toluene absorption. First, COSMO-RS method was used to analyze the solute-solvent intermolecular interactions and to screen >200 ILs, for selecting a set of optimum cation-anion combinations for toluene absorption. Absorption experiments confirmed that the selected ILs present high absorption capacities for toluene and absorption rates close to other solutes as CO_2 in ILs. The results obtained for experimental thermodynamic and kinetic data were in good agreement with theoretical predictions. Process simulation by Aspen Plus allowed concluding that thermodynamics considerations prevail in toluene absorption, but evidenced the need of considering also kinetics in the selection of the IL selection and the design of IL-based separation processes. Imidazolium-based ILs with [NTf_2] anion and high length of the cation alkyl chain are found suitable ILs for toluene absorption, considering both kinetic and thermodynamic aspects.

Table 5. Toluene Recovery (%), Toluene Molar Fraction in the Exit Gas [$y_{Toluene}$(gas out)] and Height Equivalent to a Theoretical Plate (HETP) in a 2 m Height Absorption Packed Column at 293 K, 1 atm, G/L = 17 (in mol), and $y_{Toluene}$(gas in) = 0.002, Simulated by Aspen Plus

	Toluene Recovery (% in mol)	$y_{Toluene}$ (Gas Out) (in mol)	HETP (m)
DEHA	90	$1.9 \cdot 10^{-4}$	0.77
[dcmim][NTf_2]	83	$3.4 \cdot 10^{-4}$	0.57
n-Hexadecane	73	$5.2 \cdot 10^{-4}$	1.36

Acknowledgments

The authors are grateful to the Spanish "Ministerio de Economía y Competitividad" and "Comunidad de Madrid" for financial support (projects CTQ2011-26758 and S2009/PPQ-1545). J. Bedia acknowledges the Spanish MICINN for financing his research through the "Juan de la Cierva" post doctoral program. We are very grateful to "Centro de Computación Científica de la Universidad Autónoma de Madrid" for computational facilities.

Literature Cited

1. Hunter P, Oyama ST. *Control of volatile organic compounds emissions*. In: *Conventional and Emerging Technologies*. Wiley-Interscience, New York: Wiley-InterScience, 2000.
2. Rafson HJ. *Odor and VOC Control Handbook*. USA: McGraw-Hill, 1998.
3. Milota M, Mosher P, Li L. VOCs and HAP removal from dryer exhaust gas by adsorption into ionic liquids. *Forest Products J*. 2007;57:73–77.
4. Bedia J, Rosas JM, Rodríguez-Mirasol J, Cordero T. Pd supported on mesoporous activated carbons with high oxidation resistance as catalysts for toluene oxidation. *Appl Catal B Environ*. 2010;94:8–18.
5. Solsona B, Garcia T, Aylón E, Dejoz AM, Vázquez L, Agouram S, Davies TE, Taylor SH. Promoting the activity and selectivity of high surface area Ni–Ce–O mixed oxides by gold deposition for VOC catalytic combustion. *Chem Eng J*. 2011;175:271–278.
6. Arriaga S, Muñoz R, Hernandez S, Guieysse B, Revah S. Gaseoseus hexane bidegradation by Fusarium solami in two liquid phase packed-bed and stirred-tank bioreactors. *Environ Sci Tech*. 2006;40:2390–2395.
7. Quijano G, Couvert A, Amrane A, Darracq G, Couriol C, Le Cloirec P, Paquin L, Carrié D. Potential of ionic liquids for VOC absorption and biodegradation in multiphase systems. *Chem Eng J*. 2011;66:2707–2712.
8. Chiang Y-C, Chiang P-C, Huang C-P. Effects of pore structure and temperature on VOC adsorption on activated carbon. *Carbon* 2001;39:523–534.
9. Jarraya I, Fourmentin S, Benzina M, Bouaziz S. VOC adsorption on raw and modified clay materials. *Chem Geol*. 2010;275:1–8.
10. Blach P, Fourmentin S, Landy D, Cazier F, Surpateau G, Cyclodextrins A. A new efficient absorbent to treat waste gas streams. *Chemosphere* 2008;70:374–380.
11. Wang X, Daniels R, Baker RW. Recovery of VOCs from high-volume low-VOC concentration air streams. *AIChE J*. 2001;47:1094–1100.
12. Darracq G, Couvert A, Couriol C, Amrane A, Thomas D, Dumont E, Andres Y, Le Cloirec P. Silicone oil: an effective absorbent for the removal of hydrophobic volatile organic compounds. *J Chem Technol Biotechnol*. 2010;85:309–313.
13. Wasserscheid P, Welton T. *Ionic Liquids in Synthesis*. Weinheim, Germany: Wiley-VCH Verlag GmbH & Co. KGaA, 2008.
14. Plechkova NV, Rogers RD, Seddon KR. *Ionic Liquids: from Knowledge to Application. ACS Symposium Series* 1030, American Chemical Society, Washington DC, 2009.
15. González JA, Mozo I, de la Fuente IG, Cobos JC. DISQUAC Predictions on thermodynamic properties of ternary and higher multicomponent mixtures. 3. Results for he of ternary mixtures containing one alcohol, one polar compound, and one hydrocarbon or two alcohols and one hydrocarbon or a polar compound, or three alkanols. *Ind Eng Chem Res*. 2004;43:7622–7634.
16. Palomar J, Torrecilla JS, Lemus J, Ferro VR, Rodríguez F. A COSMO-RS based guide to analyze/quantify the polarity of ionic liquids and their mixtures with organic cosolvents. *Phys. Chem Chem Phys*. 2010;12:1991–2000.
17. Giernoth R. Task-specific ionic liquids. *Angew Chem Int*. 2010;49:2834–2839.
18. Han D, Row KH. Recent applications of ionic liquids in separation technology. *Molecules* 2010;15:2405–2426.
19. Han X, Armstrong DW. Ionic liquids in separations. *Acc Chem Res*. 2007;40:1079–1086.
20. Huang J, Ruether T. Why are ionic liquids attractive for CO2 absorption? An overview. *Aust J Chem*. 2009;62:298–308.

21. Bara JE, Carliste TK, Gabriel CJ, Camper D, Finotello A, Gin DL, Noble RD. Guide to CO separations in imidazolium-based room-temperature ionic liquids. *Ind Eng Chem Res*. 2009;48:2739–2751.
22. Shiflett MB, Yokozeki A. Chemical absorption of sulfur dioxide in room temperature ionic liquids. *Ind Eng Chem Res*. 2010;49:1370–1377.
23. Ren SH, Hou YC, Wu WZ, Liu QY, Xiao YF, Chen XT. Properties of ionic liquids absorbing SO2 and the mechanism of the absorption. *J Phys Chem B* 2010;114:2175–2179.
24. Yokozeki A, Shifflet MB. Ammonia solubilities in room-temperature ionic liquids. *Ind Eng Chem Res*. 2007;46:1605–1610.
25. Palomar J, Gonzalez-Miquel M, Bedia J, Rodriguez F, Rodriguez JJ. Task-specific ionic liquids for efficient ammonia absorption. *Sep Purif Technol*. 2011;82:43–52.
26. Bedia J, Palomar J, Gonzalez-Miquel M, Rodriguez F, Rodriguez JJ. Screening ionic liquids as suitable ammonia absorbents on the basis of thermodynamic and kinetic analysis. *Sep Purif Technol*. 2012;187:115–121.
27. Shiflett MB, Yokozeki A. Solubility and diffusivity of hydrofluorocarbons in room-temperature ionic liquids. *AIChE J*. 2006;52:1205–1219.
28. Shiflett MB, Shiflett AD, Yokozekic A. Separation of tetrafluoroethylene and carbon dioxide using ionic liquids. *Sep Purif Technol*. 2011;79:357–364.
29. Ortiz A, Galan LM, Gorri D, de Haan AB, Ortiz I. Kinetics of reactive absorption of propylene in RTIL-Ag+ media. *Sep Purif Technol*. 2010;73:106–113.
30. Ortiz A, Galan LM, Gorri D, de Haan AB, Ortiz I. Reactive Ionic Liquid Media for the Separation of Propylene/Propane Gaseous Mixtures. *Ind Eng Chem Res*. 2010;49:7227–7233.
31. Klamt A, Eckert F, Arlt W. COSMO-RS: an alternative to simulation for calculating thermodynamic properties of liquid mixtures. *Annu Rev Chem Biomed Eng*. 2010;1:101–122.
32. Diedenhofen M, Klamt A. COSMO-RS as a tool for property prediction of IL mixtures—a review. *Fluid Phase Equilib*. 2010;294:31–38.
33. Palomar J, Ferro VR, Torrecilla JS, Rodriguez F. Density and molar volume predictions using COSMO-RS for ionic liquids: an approach to solvent design. *Ind Eng Chem Res*. 2007;46:6041–6048.
34. Palomar J, Torrecilla JS, Ferro VR, Rodríguez F. Development of an a priori ionic liquid design tool 1: integration of a Novel COSMO-RS molecular descriptor on neural networks. *Ind Eng Chem Res*. 2008;47:4523–4532.
35. Palomar J, Torrecilla JS, Ferro VR, Rodríguez F. Development of an a priori ionic liquid design tool 2: ionic liquid selection through the prediction of COSMO-RS molecular descriptor by inverse neural network. *Ind Eng Chem Res*. 2009;48:2257–2265.
36. Palomar J, González-Miquel M, Polo A, Rodríguez F. Understanding the physical absorption of CO2 in ionic liquids using the COSMO-RS method. *Ind Eng Chem Res*. 2011;50:3452–3463.
37. González-Miquel M, Palomar J, Omar S, Rodríguez F. CO2/N2 selectivity prediction in supported ionic liquid membranes (SILMs) by COSMO-RS. *Ind Eng Chem Res*. 2011;50:5739–5748.
38. Navas A, Ortega J, Vreekamp R, Marrero E, Palomar J. Experimental thermodynamic properties of 1-butyl-2-methylpyridinium tetrafluoroborate [b2mpy][BF4] with water and with alkan-1-ol and their interpretation with the COSMO-RS methodology. *Ind Eng Chem Res*. 2009;48:2678–2690.
39. Vreekamp R, Castellano D, Palomar J, Ortega J, Espiau F, Fernández L, Penco E. Thermodynamic behavior of the binaries 1-butylpyridinium tetrafluoroborate with water and alkanols: their interpretation using 1H NMR spectroscopy and quantum-chemistry calculations. *J. Phys Chem B* 2011;115:8763–8774.
40. Aspen Technology, Inc. *Aspen Plus v7.3*. Burlington, MA, 2010.
41. Ferro VR, Ruiz E, Tobajas M, Palomar JF. Integration of COSMO-based methodologies into commercial process simulators. Separation and purification of reuterin. *AIChE J*. 2012;58:3404–3415.
42. Ferro VR, Ruiz E, de Riva J, Palomar JF. Introducing process simulation in ionic liquids design/selection for separation processes based on operational and economic criteria through the example of their regeneration. *Sep. Purif. Technol*. 2012;97:195–204.
43. Lin ST, Sandler SI. A priori phase equilibrium prediction from a segment contribution solvation model. *Ind Eng Chem Res*. 2002;41:899–913.
44. Aspen Technology. Inc. How to use COSMO-SAC, 2004. Technical Tip ID: 113674. Available at: http://support.aspentech.com.
45. Frisch MJ, Trucks GW, Schlegel HB, Scuseria GE, Robb MA, Cheeseman JR, Montgomery JA, Vreven T, Kudin KN, Burant JC, Millam JM, Iyengar SS, Tomasi J, Barone V, Mennucci B, Cossi M, Scalmani G, Rega N, Petersson GA, Nakatsuji H, Hada M, Ehara M, Toyota K, Fukuda R, Hasegawa J, Ishida M, Nakajima T, Honda Y, Kitao O, Nakai H, Klene M, Li X, Knox JE, Hratchian HP, Cross JB, Bakken V, Adamo C, Jaramillo J, Gomperts R, Stratmann RE, Yazyev O, Austin AJ, Cammi R, Pomelli C, Ochterski JW, Ayala PY, Morokuma K, Voth GA, Salvador P, Dannenberg JJ, Zakrzewski VG, Dapprich S, Daniels AD, Strain MC, Farkas O, Malick DK, Rabuck AD, Raghavachari K, Foresman JB, Ortiz JV, Cui Q, Baboul AG, Clifford S, Cioslowski J, Stefanov BB, Liu G, Liashenko A, Piskorz P, Komaromi I, Martin RL, Fox DJ, Keith T, Al-Laham MA, Peng CY, Nanayakkara A, Challacombe M, Gill PM, Johnson B, Chen W, Wong MW, González C, Pople JA. *Gaussian03, revision B.05*, Wallingford, CT: Gaussian, Inc., 2004.
46. Eckert F, Klamt A. *COSMOthermX, Version C2.1, Release 01.11*; COSMOlogic GmbH & Co. KG., Leverkusen, Germany, 2010.
47. Ahosseini A, Scurto AM. Viscosity of imidazolium-based ionic liquids at elevated pressures: cation and anion effects. *Int J Thermophys* 2008;29:1222–1243.
48. Zhang S, Lu X, Zhou Q, Li X, Zhang X, Li S. *Ionic Liquids—Physicochemical Properties*. Amsterdam, The Netherlands: Elsevier, 2009.
49. Jacquemin J, Husson P, Padua AAH, Majer V. Density and viscosity of several pure and water-saturated ionic liquids. *Green Chem*. 2006;8:172–180.
50. Tokuda H, Hayamizu K, Ishii K, Susan Md. ABH, Watanabe M. Physicochemical Properties and Structures of Room Temperature Ionic Liquids. 1. Variation of Anionic Species. *J Phys Chem. B* 2004;108:16593–16600.
51. Carlisle TK, Bara JE, Gabriel CJ, Noble RD, Gin DL. Interpretation of CO2 solubility and selectivity in nitrile-functionalizaed room-temperature ionic liquids using a group contribution approach. *Ind Eng Chem Res*. 2008;47:7005–7012.
52. Lin ST, Sandler SI. A priori phase equilibrium prediction from a segment contribution solvation model. *Ind Eng Chem Res*. 2002;41:899–913.
53. Heymes F, Demoustier PM, Charbit F, Fanlo JL, Moulin P. Hydrodynamics and mass transfer in a packed column: case of toluene absorption with a viscous absorbent. *Chem Eng Sci*. 2006;61:5094–5106.
54. Crosthwaite JM, Muldoon MJ, Dixon JK, Anderson JL, Brennecke JF. Phase transition and decomposition temperatures, heat capacities and viscosities of pyridinium ionic liquids. *J Chem Thermodynamics* 2005;37:559–568.
55. Khupse ND, Kumar A. Dramatic change in viscosities of pure ionic liquids upon addition of molecular solvents. *J Solution Chem*. 2009;38:589–600.
56. Fraser KJ, Izgorodina EI, Forsyth M, Scott JL, MacFarlane DR. Liquids intermediate between "molecular" and "ionic" liquids: liquid ion pairs? *Chem Commun*. 2007;37:3817–3819.
57. Vuong M-D, Couvert A, Couriol C, Amrane A, Le Cloirec P, Renner C. Determination of the Henry's constant and the mass transfer rate of VOCs in solvents. *Chem Eng J*. 2009;150:426–430.
58. Brodkey RS, Hershey HC. *Transport Phenomena: A Unified Approach*, Columbus, OH: Brodkey, 2003.
59. Huang J, Riisager A, Berg RW, Fehrmann R. Tunning ionic liquids for high gas solubility and reversible gas sorption. *J Mol Catal A* 2008;279:170–176.
60. Shiflett MB, Yokozeki A. Solubilities and diffusivities of carbon dioxide in ionic liquids [bmim][PF6] and [bmim][BF4]. *Ind Eng Chem Res*. 2005;44:4453–4464.
61. Crank J. *The mathematics of diffusion*. 2nd ed. London: Oxford University Press, 1975
62. Hou Y, Baltus RE. Experimental measurements of the solubility and diffusivity of CO2 in room-temperature ionic liquids using a transient thin-liquid-film method. *Ind Eng Chem Res*. 2007;46:8166–8175.
63. Wilke CR, Lee CY. Correlation of diffusion coefficients in dilute solutions. *AIChE J*. 1955;1:264–270.

Manuscript received Mar. 19, 2012, and revision received Aug. 27, 2012.